

The DIRC-like FTOF: A Time-of-Flight Cherenkov Detector for Particle Identification at SuperB

L. Burmistrov

► **To cite this version:**

L. Burmistrov. The DIRC-like FTOF: A Time-of-Flight Cherenkov Detector for Particle Identification at SuperB. Workshop on Timing Detectors: Electronics, Medical and Particle Physics Applications, Nov 2010, Cracow, Poland. pp.91-99, 10.5506/APhysPolBSupp.4.91 . in2p3-00613224

HAL Id: in2p3-00613224

<http://hal.in2p3.fr/in2p3-00613224>

Submitted on 24 Apr 2012

HAL is a multi-disciplinary open access archive for the deposit and dissemination of scientific research documents, whether they are published or not. The documents may come from teaching and research institutions in France or abroad, or from public or private research centers.

L'archive ouverte pluridisciplinaire **HAL**, est destinée au dépôt et à la diffusion de documents scientifiques de niveau recherche, publiés ou non, émanant des établissements d'enseignement et de recherche français ou étrangers, des laboratoires publics ou privés.

THE DIRC-LIKE FTOF: A TIME-OF-FLIGHT CHERENKOV DETECTOR FOR PARTICLE IDENTIFICATION AT SUPERB*

L. BURMISTROV

Laboratoire de l'Accélérateur Linéaire
CNRS/IN2P3 and Université Paris-Sud 11, France

(Received February 4, 2011)

The DIRC-like FTOF detector is a ring imaging Cherenkov counter which uses Time-of-Flight to identify charged particles. A prototype of such device was constructed and installed in the SLAC Cosmic Ray Telescope for timing measurement. A time resolution of about 90 ps/channel was obtained, in agreement with simulation. To estimate the different contributions to the single channel time resolution, a precise simulation of the whole system (detector + MCP-PMT) was written. For this experiment we use the new 10 ps 16-channel USB wave catcher electronics developed by LAL (CNRS/IN2P3) and CEA/IRFU. In this paper, preliminary results of the test ongoing at SLAC are presented. This work is done in collaboration with N. Arnaud, D. Breton, J. Maalmi, V. Puill, A. Stocchi from LAL and D. Aston, J. Va'vra from SLAC.

DOI:10.5506/APhysPolBSupp.4.91

PACS numbers: 29.40.Ka, 29.85.Ca, 29.85.Fj

1. Introduction

The SuperB factory [1] is a project of an asymmetric energy e^+e^- collider, operating at the $\Upsilon(4S)$ resonance. The machine design is based on the new “crab-waist” scheme, successfully tested at the DAΦNE upgraded collider in 2008–2009 [2, 3]. This new scheme will allow SuperB to reach an instantaneous luminosity of $10^{36}\text{cm}^{-2}\text{s}^{-1}$ and to integrate more than 50ab^{-1} in five years of data taking. This huge dataset will allow SuperB to perform high-precision tests of the Standard Model and to probe New Physics in the flavour sector.

* Presented at the Workshop on Timing Detectors, Kraków, Poland, November 29–December 1, 2010.

The SuperB detector [1,4] will be similar to the BaBar detector [5] with some modifications required to operate at high luminosity and with a reduced center-of-mass boost ($\beta\gamma = 0.28$). Its nominal design consists of a tracking system which includes a silicon vertex tracker and a drift chamber (DCH), the FDIRC, a Cherenkov detector for charged particle identification (PID), an electromagnetic calorimeter (EMC) and an instrumented flux-return to detect muons. The FDIRC (Focusing Detector of Internally Reflected Cherenkov light) is based on the same principle than the successful BaBar DIRC [6] and will actually reuse its quartz bars. It covers the barrel region and provides very good K/π separation in the 0.8–4.0 GeV/ c momentum range. There are currently proposals to add another PID detector on the forward side of SuperB, between the DCH and the forward EMC. One of the main candidates for this forward PID system is the FTOF (Forward Time-of-Flight) detector.

The main goal of the forward PID detector is to improve the K/π separation in the 0.8–3.0 GeV/ c momentum range, in a polar region only covered by the DCH in the BaBar/nominal SuperB design. The main requirements for one such device are the following: small radiation length (X_0), compact (limited space between the DCH and the forward EMC) and radiation hardness. A DIRC-like FTOF detector with a 30 ps time resolution would achieve all these goals.

2. Current status of the DIRC-like TOF studies

The FTOF measures the particle Time-of-Flight (TOF) to separate kaons from pions. The start time is given by the bunch crossing while the detection of Cherenkov photons produced by the charged tracks while crossing a quartz volume provides the stop time for the TOF measurement. The FTOF is based on the same principle as the BaBar DIRC. The detector material (quartz) is used in two ways: first as a Cherenkov radiator, then as a light guide for the Cherenkov light trapped in the radiator by total internal reflection — see Fig. 1. Unlike for the DIRC, the Cherenkov angle is not measured by the FTOF: what matters is the arrival time of the photons in the photo-multiplier (PMT) channels.

The overall detector is made of 12 quartz sectors with thickness 15 mm (about 15% X_0) covering 30° in azimuth each. The Cherenkov light produced is detected by Hamamatsu SL10 [7] multi-channel plate (MCP)-PMTs: 14 per sector, hence 168 in total — see Fig. 1. The FTOF is a 2-dimensional device: both the time and the position of the hits in the MCP-PMTs are needed to perform PID. The FTOF will be located about 2 meters away from the SuperB interaction point; hence it will cover a [15°; 25°] range in polar angle.

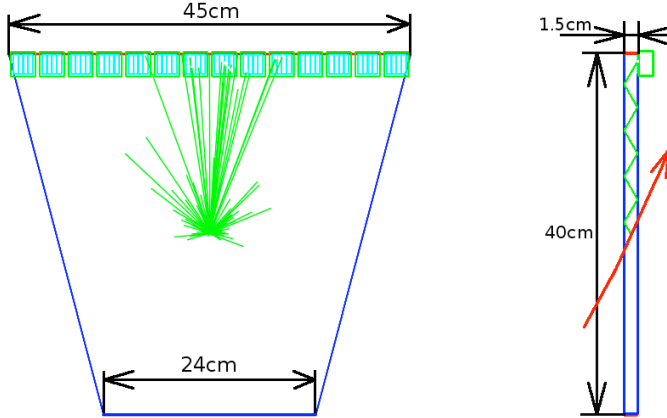


Fig. 1. (Left) Front view of one FTOF sector; the 14 MCP-PMTs are connected to the outer side of the quartz tile and Cherenkov photons are shown in grey (green). (Right) Side view of the same sector; the charged track crossing the quartz is indicated by the (red) arrow; an example of Cherenkov photon path is shown as well in grey (green).

The total time resolution can be estimated using the following formula:

$$\sigma_{\text{tot}}^2 \sim \left(\frac{\sigma_{\text{electronics}}}{\sqrt{N_{\text{p.e.}}}} \right)^2 + \left(\frac{\sigma_{\text{detector}}}{\sqrt{N_{\text{p.e.}}}} \right)^2 + \left(\frac{\sigma_{\text{TTS}}}{\sqrt{N_{\text{p.e.}}}} \right)^2 + \sigma_{\text{trk}}^2 + \sigma_{t_0}^2, \quad (1)$$

where $N_{\text{p.e.}}$ is the number of photo-electrons (p.e.) which depends on the track parameters (mass, momentum and angles with respect to the quartz tiles). A full Geant4 [8] simulation of the FTOF shows that $N_{\text{p.e.}}$ is at least 9 (18) for 0.8 GeV/c (2 GeV/c) kaons. σ_{detector} is the time spread coming from the detector (chromaticity, different photon paths, *etc.*), about 90 ps according to the full FTOF simulation. $\sigma_{\text{electronics}}$ comes from the electronics accuracy. σ_{TTS} is the transit time spread (TTS) of the MCP-PMT (35 ps for SL10). σ_{trk} is due to the track parameter reconstruction (at most 20 ps for 0.9 GeV/c kaon). σ_{t_0} is the time start resolution, dominated by the bunch-crossing time (about 20 ps).

3. Test at SLAC

A prototype of the DIRC-like FTOF has been built at the SLAC Cosmic Ray Telescope (CRT) [9] last Fall. The goals of this experiment are twofold: first, to validate the FTOF layout and then to test the performances of a electronics crate containing 8 USB WaveCatcher (USBWC) 2-channel boards [10]. During the first 4 months of data taking we collected 8×10^5 cosmic muons. The experimental setup is shown in Fig. 2.

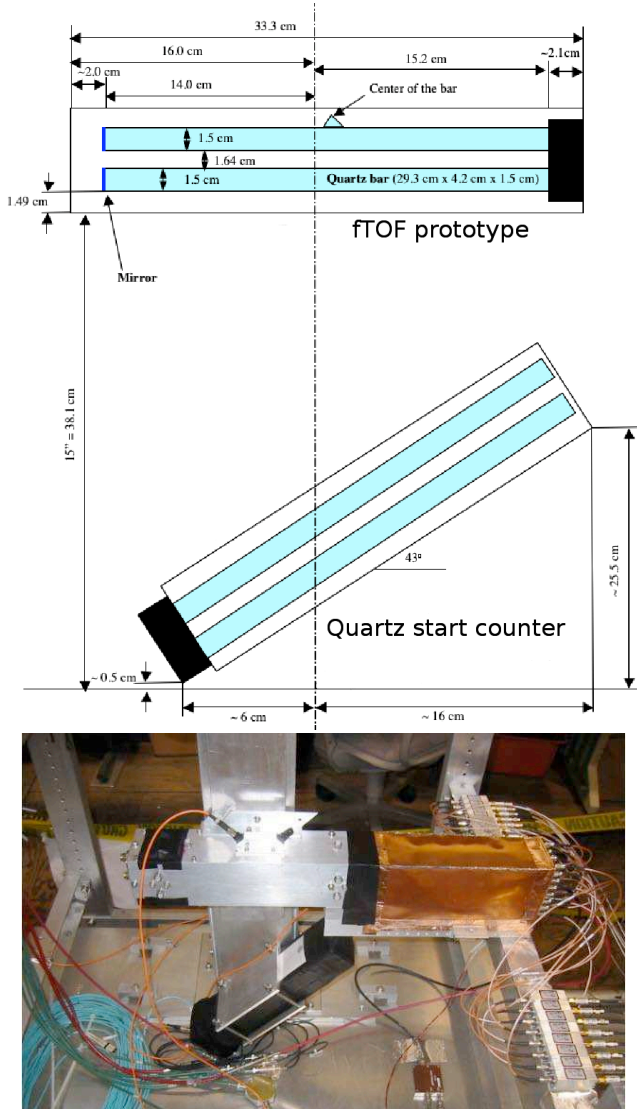


Fig. 2. (Top) The FTOF prototype (top part of the picture) is working in coincidence with a quartz start counter located under it and providing a fast trigger when a muon crosses the CRT. (Bottom) Picture of the experimental setup: the FTOF prototype is inside the aluminum box visible on the left; right to it, there is a Faraday cage (orange box) protecting the MCP-PMT from external electromagnetic noise. There are 16 PMT outputs, each connected to an USBWC electronics channel — see text for details. Under the FTOF device, one can see the quartz start counter.

3.1. Experimental setup, CRT

The two quartz bars (29.2 cm×4.2 cm×1.5 cm) are connected on one side to a Photonis 10 micron holes MCP-PMT with a 6 mm stepped face, as shown in Fig. 3. The PMT is operating at -2.7 kV which corresponds to a gain of 7×10^5 . 16 independent channels are defined from the 8×8 -pixel matrix of the PMT using the following scheme. The top three pixels of a given column are connected together to form one channel. Going down, the next two pixels are grounded and the bottom three form another channel. The same pattern is reproduced on all 8 columns and allows the top and bottom channels to be clearly separated. Each channel is connected to a 600 MHz bandwidth filter, followed by a 500 MHz bandwidth amplifier with a 40 dB gain and finally to an USBWC channel. Events are saved to disk each time there is a coincidence between the quartz start counter and one of the USBWC channels (which common threshold is set to 20 mV). Each of the 16 waveforms has a length of 256 points separated in time by 312.5 ps.

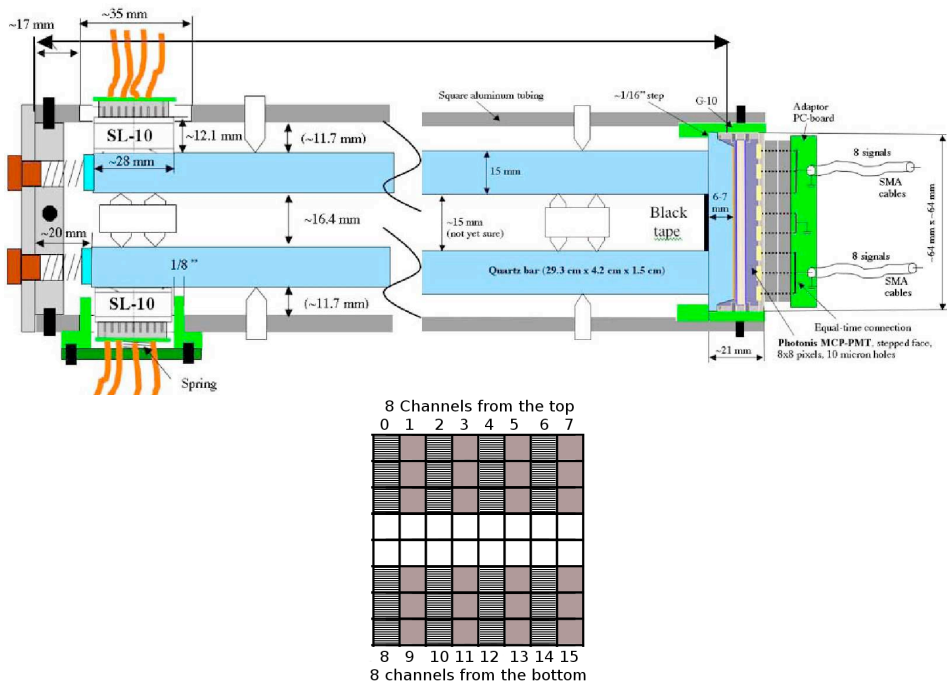


Fig. 3. (Top) Side view of the FTOF prototype showing the two quartz bars connected to the MCP-PMT on the right. Two mirrors are located on the left side to reflect the incoming photons backward. The setup has been designed to allow one to connect two SL10 MCP-PMTs on that side, should the current configuration be upgraded in the future. (Bottom) Schematic view of the MCP-PMTs pixels.

3.2. Simulation

The whole detector chain (geometry, PMT and electronics) is simulated. The propagation of the Cherenkov light inside the quartz bars is done in Geant4. The quantum efficiency of the bi-alkali photocathode, the PMT collection efficiency (set to 42% in order to match the data) and a 35 ps TTS are included in the simulation, such as the optical properties of the quartz (absorption length, polishing quality and dispersion). The Zenith angular (θ) distribution of the cosmic muons is parameterised like $(\cos \theta)^{1.85}$ [11]. A test run using a 635 nm laser with a low flux of photons provided information on the single p.e. detector response, which was then used to simulate waveforms. The template for a single p.e. waveform is the average shape of the signals recorded during this laser run — see Fig. 4 (left). Its amplitude is randomly drawn from the distribution shown in Fig. 4 (right). The number of p.e. per channel (3 in average) and their arrival times are taken from the Geant4 simulation. In case of multiple p.e., the total waveform is the sum of all individual waveforms. Finally, white noise with a 1.5 mV RMS (the level measured with the real system) is added to the generated signal.

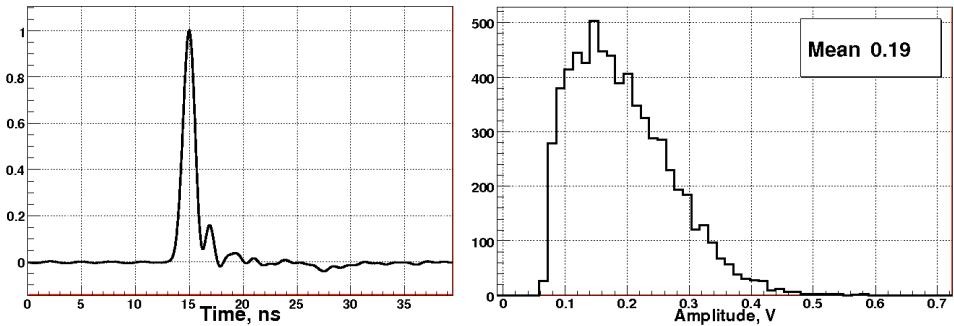


Fig. 4. (Left) Average MCP-PMT signal shape from single photo-electron. (Right) Corresponding distribution of the signal amplitudes.

As shown in the left plot in Fig. 5, photons from a given muon track can arrive at various times due to different possible paths. Each of the peaks in the black histogram corresponds to a different ‘population’ of photons. The right plot demonstrates that the effect of multiple p.e. must be taken into account as the next photons are likely to arrive within the rise time of the signal coming from the first photon.

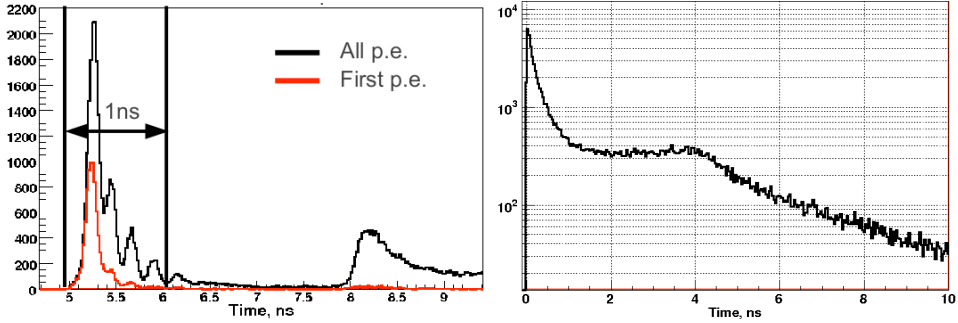


Fig. 5. (Left) Simulated distribution of the p.e. arrival time in channel No. 3 (the time origin is arbitrary) including all p.e. (black histogram) or selecting only the earliest one (red histogram). These histograms correspond to one particular set of parameters for the incoming muon track. (Right) Histogram of the photon arrival time in channel No. 3; here, the time origin corresponds to the arrival of the earliest photon (when at least two photons reach this channel in the same event) and the first bin at 0 is not displayed. Note the logarithmic scale: when there are more than 1 p.e., the following hits are very likely to arrive within the PMT rise time, hence impacting the shape of the waveform signal and making the determination of the p.e. arrival time less accurate.

3.3. Data analysis

The waveform analysis starts with a 3rd-order spline interpolation. It provides 5 additional equidistant points between two consecutive USBWC values which are then joined by lines. 5 parameters can be computed for each waveform. The amplitude of the signal, taken from the first peak exceeding a 70 mV threshold. The signal time corresponding to a constant fraction of 50% from the amplitude (cft_{50}). The signal charge, proportional to the integral of the waveform. The signal rise time, defined as the difference $cft_{90} - cft_{10}$. A shape classification number (shapeID) is used to identify clean waveforms suitable for time measurements. In this analysis we define three categories of waveforms. Signals which start with a negative edge have $\text{shapeID} = 0$ and are called ‘crosstalk-like’; ‘single peak’ signals ($\text{shapeID} = 1$) start with a positive edge and only have one peak. Finally, ‘multippeak-like’ signals — which start with a positive edge and present at least 2 peaks — have $\text{shapeID} = 2$. Since we do not know precisely the start time of the event, we construct time differences between neighbour channels. We require three conditions in order to choose good waveforms: $\text{shapeID} = 1$ and $0.9 \text{ ns} < \text{rise time} < 1.2 \text{ ns}$ (see Fig. 6, right) for both channels, plus the difference between their rise times to be within $\pm 0.15 \text{ ns}$.

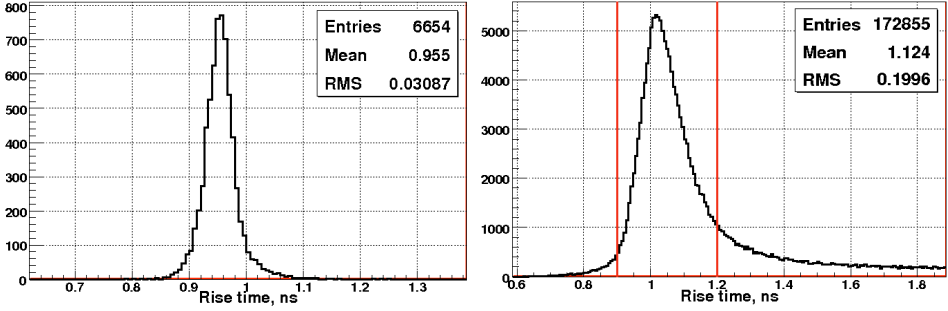


Fig. 6. Distribution of the measured rise times: (Left) for single p.e. waveforms from the laser run; (Right) for signals from cosmic muons with shapeID = 1.

3.4. Simulation/Data comparison, discussion of the results

The distributions of the time difference between channels No. 2 and No. 3 are shown in Fig. 7, for simulation (left plot) and data (right plot). These histograms are fit by the sum of two Gaussians to separate their two main components. The narrow peak is due to the time differences of photons from the same ‘population’ while the wide tails arise from differences between photons of different populations — see Sec. 3.2 for details. Simulation and data are in good agreement for the widths of the Gaussians but there are still some discrepancies between their relative weights. They may be due to effects such as cross-talk and charge sharing which are not simulated yet. The dominant contribution to the time accuracy for this particular setup is coming from the multiple p.e. (3 in average per channel): about 70 ps. This effect was not anticipated when designing this test in the CRT but simulation allowed us to understand it.

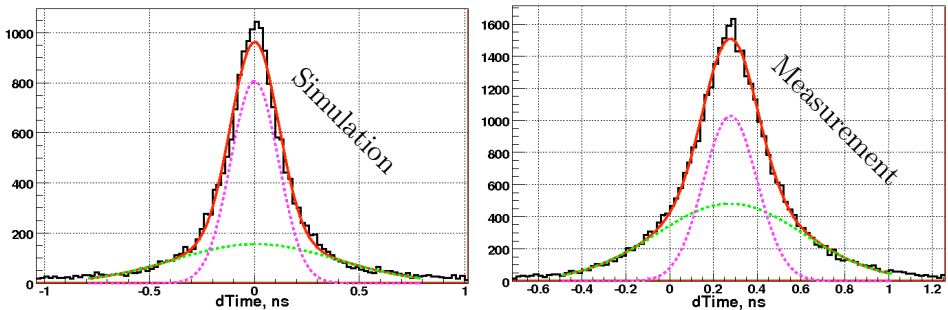


Fig. 7. Fit of the time differences between channels No. 2 and No. 3 with the sum of two Gaussians. (Left) Simulation: $\sigma_{\text{narrow}} = 113$ ps, $\sigma_{\text{wide}} = 385$ ps, $\text{fraction}_{\text{narrow}} \sim 40\%$, $\text{fraction}_{\text{wide}} \sim 60\%$. (Right) Measurements: $\sigma_{\text{narrow}} = 123$ ps, $\sigma_{\text{wide}} = 337$ ps, $\text{fraction}_{\text{narrow}} \sim 55\%$, $\text{fraction}_{\text{wide}} \sim 45\%$.

4. Conclusion and future plans

The test at SLAC CRT facility described in this article shows that a timing accuracy at the level of 90 ps per channel can be achieved with a setup similar to the FTOF detector. It also shows how important a detailed simulation is, to understand how the experimental results depend on the many parameters, among which the photon path ambiguities and the photon yield per channel.

The CRT and USBWC data acquisition systems are currently separated. Therefore, time coincidences between events seen in both detectors are needed to select waveforms produced by energetic muons which are well-reconstructed in the CRT. Including such requirement would allow us to perform a more complex analysis on a cleaner sample of events. But so far the efficiency of the matching between the two independent systems has been low — for reasons still being investigated — and so this technique has not been used yet, in order to keep enough events. We are still taking data in order to improve our understanding of the system. One recent change has been to put absorbers in front of the MCP-PMT to reduce by a significant factor the photon yield by channel. These new data are being analysed now. Finally, we may upgrade the experimental setup in the future, by adding two SL10 PMTs (with faster rise time) on the left of the bars.

REFERENCES

- [1] SuperB CDR, [arXiv:0709.0451v2](https://arxiv.org/abs/0709.0451v2) [hep-ex].
- [2] M. Zobov *et al.*, *Phys. Rev. Lett.* **104**, 174801 (2010).
- [3] M. Boscolo *et al.*, *Nucl. Instrum. Methods* **A621**, 121 (2010).
- [4] E. Grauges *et al.*, [arXiv:1007.4241](https://arxiv.org/abs/1007.4241) [physics.ins-det].
- [5] B. Aubert *et al.*, *Nucl. Instrum. Methods* **A479**, 1 (2002).
- [6] I. Adam *et al.*, *Nucl. Instrum. Methods* **A538**, 281 (2005).
- [7] K. Inami *et al.*, *Nucl. Instrum. Methods* **A592**, 247 (2008).
- [8] <http://geant4.web.cern.ch/geant4>
- [9] J. Va'vra, SLAC Cosmic Ray Telescope Facility, SLAC-PUB-13873, 2010.
- [10] D. Breton, E. Delagnes, J. Maalmi, Topical Workshop on Electronics for Particle Physics, 2009, <http://hal.in2p3.fr/in2p3-00421366/en/>
- [11] P.K.F. Grieder, *Cosmic Rays at Earth*, Elsevier, 2001.